A Single LED Photoplethysmography-based Noninvasive Glucose Monitoring Prototype System

Aminah Hina, Hamza Nadeem, and Wala Saadeh
Department of Electrical Engineering
Lahore University of Management and Sciences (LUMS)
Lahore, Pakistan
wala.saadeh@lums.edu.pk

***Abstract*— Continuous glucose monitoring is essential for patients to avoid complications of both hypoglycemia and hyperglycemia. This paper presents a novel non-invasive continuous blood glucose monitoring system based on a single wavelength near-infrared (NIR) spectroscopy. The analog frontend of the system is designed with a single NIR LED to record the Photoplethysmographic (PPG) signal from the fingertip with motion artifacts removal and a bias current rejection up to 20uA. The proposed digital backend extracts 10 discriminating features from the PPG signal to predict the blood glucose level using (Exponential Gaussian Process) machine learning regression. To realize the feature extraction on FPGA, a novel two-dimensional structure of 256-point Fast Fourier Transform (FFT) is implemented which achieves a 47% reduction in complex multiplications compared to the conventional Radix-2 algorithm. The performance of the proposed system is validated using 200 patients PPG recordings and glucose levels measured via a commercial glucometer. It successfully predicts the glucose level with a mean absolute relative difference (mARD) of 8.97%.**

Keywords*— Glucose Monitoring, wearable devices, machine learning, regression, NIR.

I. INTRODUCTION

Diabetes can be considered as one of the most globally prevalent diseases with ~415 million patients [1]. Diabetic patients and pregnant women suffering from gestational diabetes are required to continuously monitor their blood glucose level (BGL) to avoid the complications of very high or very low blood sugar. However, the conventional method of "finger-stick" that measures the sugar level by taking blood samples is painful and not comfortable for patients for frequent usage. A more viable approach is to utilize a non-invasive glucose monitoring that continuously measures BGL with no pain or discomfort. Various non-invasive glucose monitoring systems were proposed based on different techniques such as multi-wavelength near-infrared spectroscopy, impedance spectroscopy, and other optical methods [2]-[4]. Impedance spectroscopy identifies variations in the electrical properties of the human tissue affected by BGL, however, this method requires the use of multiple electrodes and the contact impedance between skin and electrodes can deteriorate the measurement [2], [5].

Near-infrared (NIR) spectroscopy is a promising optical method that has been adopted in developing non-invasive glucose monitoring systems [4]-[9]. It is based on penetrating light with a wavelength of 700-2500 nm through the patient skin such as fingertip or earlobe and recording the received light signal. The absorption of the optical signal by muscles, skin tissue and venous blood remains constant in short time while variations in arterial blood will introduce changes in the light intensity periodically forming Photoplethysmography (PPG) signal [9]. Changes in blood viscosity and vessel compliance are related to the BGL [8]-[11]. Several studies analyzed the PPG signal from multi-wavelength LEDs and extracted physiological parameters of human blood to estimate BGL [10], [11]. However, these systems are not optimal for the wearable environment since the LED drivers typically have a high power consumption that can reach up to tens of mWs for each LED [4], [12].

This paper proposes a non-invasive glucose monitoring system that uses a single NIR LED (940nm) to acquire the PPG signal, and extract 10 discriminating features with an exponential Gaussian process regression (GPR) model to predict the BGL values. The proposed system is the first system that implements a single wavelength NIR spectroscopy for BGL monitoring on- a field-programmable gate array (FPGA). It proposes a two-dimensional structure of 256 Fast Fourier Transform (FFT) to realize feature extraction on FPGA with minimum energy and area usage.

II. PROPOSED GLUCOSE MONITORING SYSTEM

The block diagram of the proposed BGL monitoring system can be decomposed into three main modules as shown in Fig. 1. The first module consists of a clip and PPG analog front-end, which acquires the PPG signals, implemented on Printed Circuit Board (PCB). The index finger is placed in a clip that comprises of NIR LED and a photodiode. When light penetrates through the finger tissue, the photodiode generates a current directly proportional to the fluctuations in light intensity. The LED brightness is kept constant such that the variation in light intensity is only due to the blood flow in the finger. The photodiode current is fed to a trans-impedance amplifier (TIA) that converts the input current to voltage and then the output voltage signal is passed to a DC current removal (DCR) circuit. DCR removes the DC offset caused by ambient light and respiration signal distortion. The signal is then amplified and filtered. Programmable gain amplifier (PGA) is utilized for further amplification and offset addition. This is required by the FPGA to digitize the signal and process it.

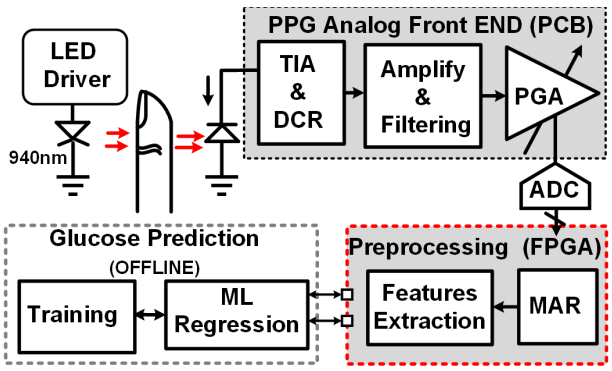

Fig. 1: Block Diagram of the Proposed BGL Monitoring System.

978-1-7281-0397-6/19/$31.00 ©2019 IEEE

In the second module, the preprocessing of signal and feature extraction are implemented on FPGA, where baseline drift and noises due to motion artifacts are mitigated. After noise reduction, the PPG signal is fragmented and features are extracted from the frames. The third module predicts BGL using machine learning exponential GPR model. In the current implementation, Glucose estimation and training are performed offline using Matlab Statistics and Machine Learning Toolbox Apps.

III. PPG Analog Front End

The PPG signal analog frontend is composed of NIR LED and photodiode with signal conditioning circuits. As a light source, NIR LED (TSAL5300) with λ= 940nm is used. This wavelength is selected since it is largely absorbed by glucose while being transparent to water [13]. The FGA10 (Thorlabs photodiode) is used to detect the transmitted light since it has a high spectral response from λ=700nm-1800nm. The photodiode typically has a bias current range of 4nA to 10uA with an AC component of 0.5%-2% of the bias current [13].

Fig. 2 shows the schematics of the PPG signal readout circuit where the low photodiode current is converted to a voltage using a TIA circuit with a gain of 1MΩ formed by the feedback resistor. A passive RC HPF with a cut-off of 0.04Hz is utilized to reject the DC component, which allows for a maximum bias current of 20uA in the photodiode current. After removing offset, the signal is amplified with a gain of 20dB. Further amplification is implemented in the next stage after passing the signal through an active bandpass filter (BPF) (0.07-5 Hz). The output of BPF is also amplified using an amplifier of gain 40dB. The PPG signal is further filtered through an RC LPF with a cutoff of 15 Hz to remove high-frequency noises. The final stage is PGA (20-40dB) which adds the desired offset and amplifies the PPG signal before the analog-to-digital conversion (ADC) in the FPGA.

IV. Glucose Estimation Digital Backend

The signal preprocessing is implemented on FPGA. First, the ADC block digitized the PPG signal. ADC in FPGA is of 16-bit and samples at a rate of 100S/s. Fig. 3 shows the block diagram of the glucose estimation processor. The signal from the ADC is preprocessed to mitigate motion artifacts and baseline drift. Wavelet transformation is used for PPG signal preprocessing [13]-[15].

This method has the advantage of removing baseline drifts and de-noising the signal effectively without changing its resolution in both frequency and time domain. Wavelet transformation uses different wavelets for decomposing and reconstructing of the signal through scaling and shifting operation. Wavelet function can be chosen according to the signal application. In this work, a Discrete Wavelet Transform (DWT) for PPG signal preprocessing is adopted. Daubechies wavelet (db4) is chosen for PPG signal representation [16]. Fig. 4 shows the original PPG signal with baseline drift and after applying the wavelet transformation, baseline drift has been removed.

The PPG signal, represented by $S_p(t)$ is then divided into frames $S_f(\tau, n)$ where index τ is the number of samples in a frame and n is the number of frames. The number of samples in each frame is taken to be L_{frame}= 200 and the total number of frames are n =20. There are no overlaps in the frames. The frames are then processed for feature extraction. The feature extraction module extracts the features and forms a vector X_F that is input into the machine-learning module. Training is done using different machine learning algorithms and five of them are selected for comparison. Rest of the techniques have not been selected as they showed many variations in the predicted values.

The selected models are linear regression, support vector machine (linear), support vector machine (quadratic), ensemble bagged trees and exponential GPR. Exponential GPR predicted the glucose values with minimum error and therefore this model has been selected to estimate BGL of test data. Table I shows the performances of these five techniques on the test data in terms of mean absolute difference (mARD), and Root Mean Square Error (RMSE). Exponential GPR achieves minimum error performance compared to all other techniques.

The features that are extracted from PPG signal formulate an input vector X_F into machine learning algorithm. The extracted features are described below [18].

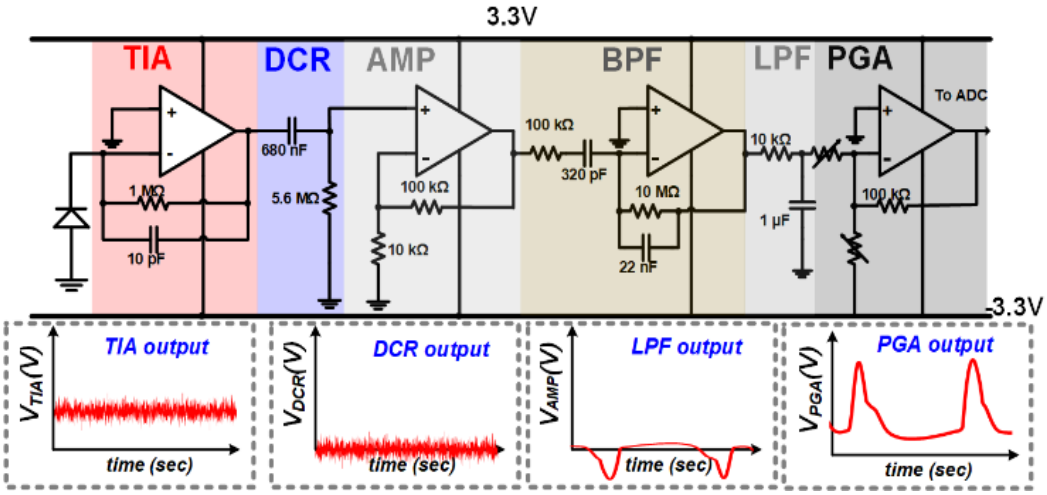

Fig. 2: The schematics of PPG readout circuit.

A. *Logarithmic Energy feature*

Logarithmic Energy (Log E_p) compute the full band spectrum energy of the PPG signal at the frame level. It is computed as follow:

$$LogE_p \leftarrow \sum_{\tau=1}^{L_{frame}} S_f^2(\tau, n) \quad (1)$$

The variance Log^{σ} and interquartile range $logE^{iqr}$ of the S_p (t) is then obtained.

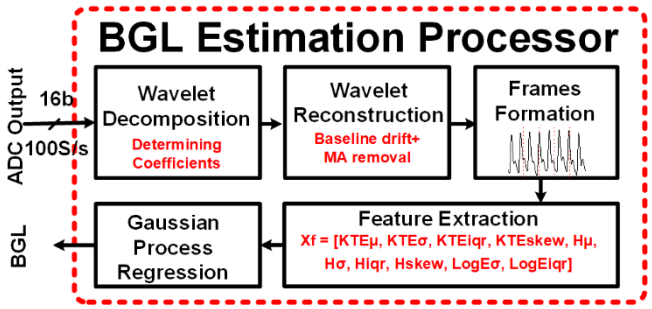

Fig. 3: Glucose Estimation digital Back End

B. *Kaiser-Teager energy feature*

The Kaiser-Teager energy (KTE) is a useful method used in signal processing for determining the energy profile of signals and endpoint detection [18]. Kaiser-Teager energy feature is obtained at the frame level using the following equation:

$$KTE_n(\tau) = S_f^2(\tau, n) - S_f(\tau + 1, n) \times S_f(\tau - 1, n) \quad (2)$$

for $\tau = 2, 3 \ldots L_{frame} - 1$

From $KTE_n(\tau)$ we compute the mean KTE^{μ}, variance KTE^{σ} interquartile range KTE_n^{IQR} and skewness KTE_n^{skew} of each frame as depicted in Fig. 5. Thus, we can compute the mean, variance, interquartile range and skewness of $S_p(t)$ by averaging the above mentioned variables.

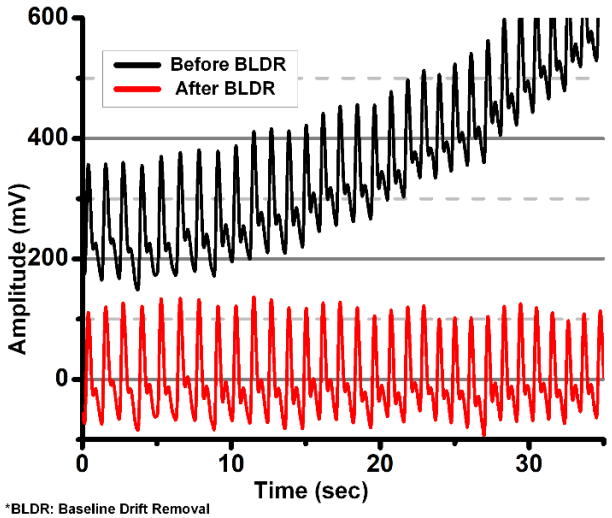

Fig. 4: PPG signal before and after baseline drift removed.

TABLE I: Comparision between different Machine Learning Algorithm.

Machine Learning Algorithm	mARD	RMSE
Linear Regression	12.06	16.2
SVM Linear	12.74	20.24
SVM Quadratic	12.30	17.97
Ensemble Bagged Trees	12.51	17.98
GPR Exponential	8.97	12.49

C. *Spectral Entropy feature*

The spectral entropy (SE) of a signal is a measure of its spectral power distribution. This feature measures the spectral shape, damping of pulses and harmonic components. It is computed by first applying FFT to each frame $S_f(\tau, n)$ of length L_{frame}, which is zero padded to expand the length to nearest power-of-two. The new length of the zero padded frame is $L_{FFT} = 256$.

$$X_n \leftarrow FFT(S_f(\tau, n)L_{FFT}) \quad (3)$$

We then normalize the squared absolute value of each FFT bin:

$$P_X^n[k] \leftarrow \frac{|X_n[k]|^2}{\sum_{j=1}^{L_{FFT}} |X_n[j]|^2}, k = 1,2 \ldots L_{FFT} \quad (4)$$

Now calculating the Entropy H_S from $P_X^n[k]$:

$$H_s \leftarrow \sum_{k=1}^{L_{FFT}} P_X^n[k]\, Log\, (P_X^n[k]) \quad (5)$$

The mean H^{μ}, variance H^{σ}, interquartile range H^{IQR} and skewness H^{skew} of $S_p(t)$ are obtained.

The input feature vector X_F is obtained by aggregating the features mentioned above.

$$X_F = [KTE^{\mu}, KTE^{\sigma}, KTE^{IQR}, KTE^{skew}, H^{\mu}, H^{\sigma}, H^{IQR}, H^{skew}, LogE^{\sigma}, LogE^{IQR}]^T \quad (6)$$

The mentioned features heavily rely on FFT computation, therefore, a 256-point hardware-efficient FFT is required. The state-of-the-art Cooley–Tukey Radix-2 FFT algorithm implementation uses >500 complex butterfly operations for 256-point FFT [22].

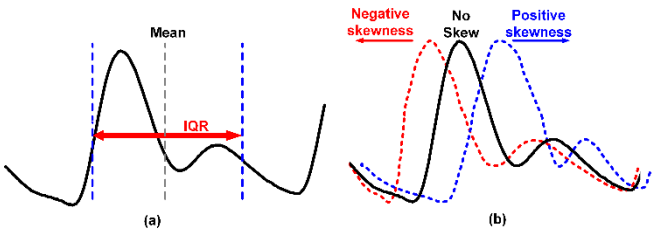

Fig. 5: PPG signal showing a) mean and interquartile (IQR) range and b) positive and negative skewness

To achieve an area-power optimization, a 256-point FFT accelerator is proposed which efficiently utilizes the 2D-structure of two (16-point FFT) and constant multiplications which decreases the required number of complex

multiplications by 69%. The proposed accelerator implementation achieves a significant reduction in area, and power, compared to the state of the art implementations [19], [22]. To realize an efficient hardware implementation of the constant multiplications, Power-of-Two Decomposition Constant (P2DC), and P2DC multiplication (P2DCM) are adapted. The constant multiplications are performed by using Addition-and-Subtraction operations, which reduces gate count by 47% [23]. The output of P2DCW fed into the 2nd 16-point FFT to evaluate the final output. The final output is ready in 32 clock cycles only, as shown in Fig. 6.

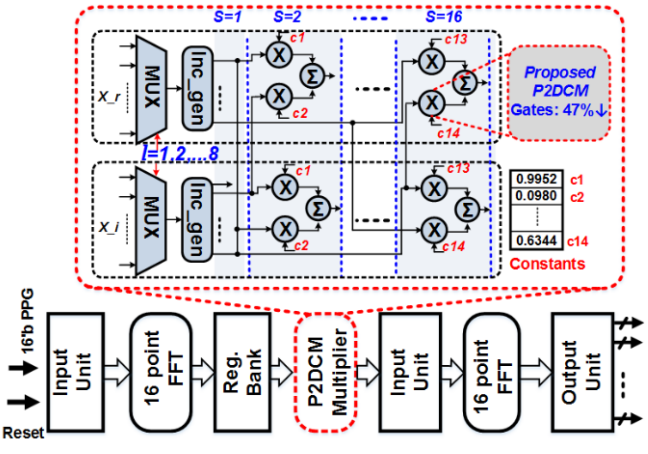

Fig. 6: 256-point FFT implementation with the proposed P2DCM block for area-energy efficient multiplication.

V. Implementation Results and Discussion

In order to validate the performance of the proposed system, the PPG signal and glucose readings were collected from 200 volunteers (men and women: age (18 to 71) years) including 4 diabetic patients. The recording process was approved by the Institutional Review Board (IRB) of our institute. The participants' PPG signal was measured from the designed PPG analog front-end. Since motion artifacts greatly affect the quality of the PPG signal, the volunteers have been asked to relax and sit comfortably prior to giving the samples. Their hands have been rested in a position to minimize movement and the fingertip has been carefully placed inside the clip. In the validation process, 80% of the recordings are used for training and 20% for testing. Fig. 7 shows the experimental setup. The finger clip is capturing PPG signals from the volunteer, the signal is processed and features are extracted on FPGA. The extracted features are sent into the system and exponential GPR model predicts the BGL. In order to verify the proposed algorithm, comparison of proposed algorithm results with goal standard is required. Therefore, off-the-shelf home use Accu-Chek instant S (Roche Pakistan Limited) blood glucose meter has been used to make reference glucose measurements. To demonstrate the accuracy of the proposed estimation, Clarke error grid (CGE) analysis is performed as shown in Fig. 8. 97.5% of estimated glucose values lie in region A, which is considered clinically acceptable zone and with mARD of 8.97%. Table II compares the performance of the proposed system with the state-of-art work for non-invasive BGL monitoring. The proposed system reduces mARD compared to multi-wavelength and different spectroscopies systems at the cost of complex hardware implementation.

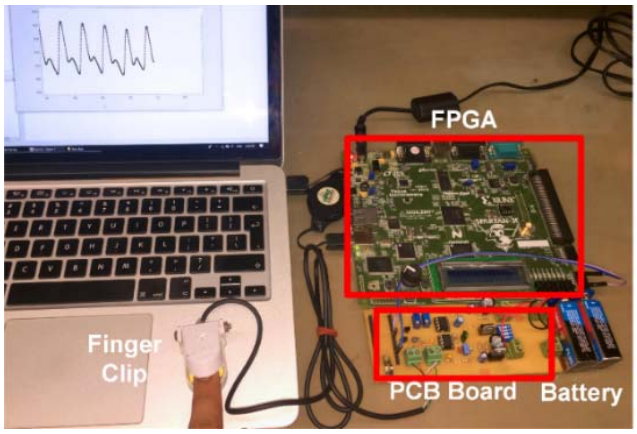

Fig. 7: Experimental set up of the proposed prototype

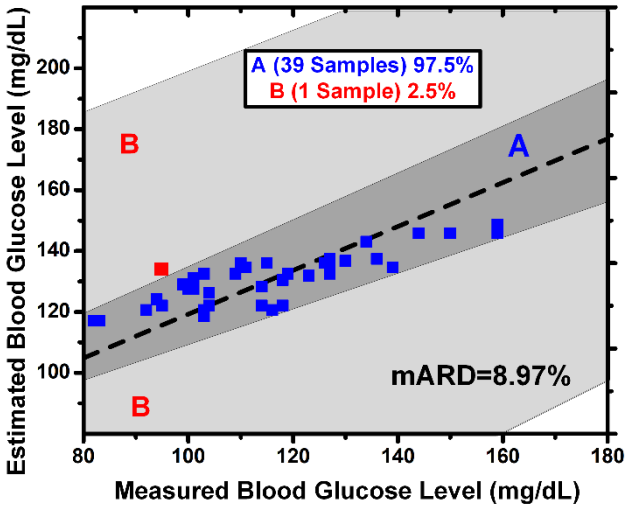

Figure 8: The Clarke error grid analysis of estimated and reference BGL (mg/dl).

TABLE II: Comparison with state of the art works.

	P. Pai EMBC'15 [13]	Z. Geng, Nature'17 [21]	Y. Zhang, ITOEC'17 [20]	K. Song JSSC'15 [4]	This Work
Technology	Multi NIR	Multi NIR and other sensors	Multi NIR	Multi-NIR and Impedance	NIR with GPR exponential
mARD	9.61%	14.4%	-	8.3%	8.97%
RMSE	-	-	1.58	-	12.49
Number of features	8	-	22	4	10
Number of patients	30	9	18	10	200
Hardware implementation	x	x	x	O	FPGA

VI. Conclusion

A non-invasive BGL monitoring system using a single NIR LED is implemented. The glucose values are predicted by extracting 10 discriminating features from PPG signal using an analog front end and an exponential GPR. The preprocessing and feature extraction model have been implemented on FPGA. A two-dimensional 256-point FFT is implemented on FPGA with a 69% reduction in complex multiplications compared to the radix-2 algorithm. The proposed system is validated using 200 subject recordings with mARD of 8.97%.

REFERENCES

[1] IDF DIABETES ATLAS, Seventh Edition, 2015, [Online]. Available: https://www.idf.org/e-library/welcome.html.

[2] A. Tura, A. Maran and G. Pacini, "Non-invasive Glucose Monitoring: Assessment of technologies and devices according to quantitative criteria," *Diabetes Res. Clinical Practice*, vol. 77, no. 1, pp. 16–40, July. 2007.

[3] A. Caduff, F. Dewarrat, M. Talary, G. Stalder, L. Heinemann, and Yu. Feldman, "Non-invasive glucose monitoring in patients with diabetes: A novel system based on Impedance Spectroscopy," *Biosens. Bioelectron*., vol. 22, no. 5, pp. 593–604, Dec. 2006.

[4] K. Song, U. Ha, S. Park, J. Bae, and H.-J. Yoo, "An Impedance and Multi-Wavelength Near-Infrared Spectroscopy IC for Non-Invasive Blood Glucose Estimation", *IEEE Journal of Solid-State Circuits*, vol. 50, no. 4, pp. 1025-1037, Apr. 2014..

[5] S. Abubakar, W. Saadeh, and M. A. B. Altaf, "A Wearable Long-Term Single-Lead ECG Processor for Early Detection of Cardiac Arrhythmia," *IEEE/ACM Design, Automation and Test in Europe (DATE)*, Mar. 2018, pp. 961-966.

[6] R.A Buda and M. M. Addi "A portable Non-invasive blood glucose monitoring device," *IEEE Conference on Biomedical Engineering and Sciences*, December 2015, pp. 964-969.

[7] R. Hotmartua, P. W. Pangestu, H. Zakaria and Y. S. Irawan, "Non-invasive blood glucose detection using near infrared sensor," *The 5th Internation Conference on Electrical Engineering and Informatics, IEEE*, August. 2015, pp. 687-692.

[8] J. Yadav, A. Rani, V. Singh, and B. M. Murari, "Near-infrared LED-based non-invasive blood glucose sensor," International Conference on Signal Processing and integrated networks (SPIN)," *IEEE*, February. 2014, pp. 687-692.

[9] S. Haxha and J. Jhoja, "Optical-based noninvasive glucose monitoring sensor prototype," *EEE Photonics Journal*, vol. 8, no. 6, pp.1-11, December. 2016.

[10] E. Mohamed, "On the analysis of fingertip photoplethysmogram signals," *Current Cardiology Reviews*, vol. 8, no. 1, February. 2012.

[11] P. Fan, H. Peiyu, L. Shangwen, and D. Wenfeng, "Feature extraction of photoplethysmography signal using Wavelet Approach," *IEEE International Conference on Digital Signal Processing (DSP)*, July. 2015, pp. 283-286.

[12] W. Saadeh, T. Habte, and M. Perrott, "A > 89% efficient LED driver with 0.5V supply voltage for applications requiring low average current," *IEEE Asian Solid-State Circuits Conference (A-SSCC)*, pp.273-276, Nov. 2013.

[13] P. P. Pai, P. K. Sanki, A. De and S. Banerjee, "NIR photoacoustic spectroscopy for non-invasive glucose measurement," *IEEE EMBC,* August. *2015*, pp. 7978-7981.

[14] G. V. Martínez, C. Alvarado-Serrano, and L. Leija-Salsas, "ECG baseline drift removal using discrete wavelet transform," *IEEE 8th International Conference on Electrical Engineering, Computing Science and Automatic Control,* October. 2011, pp. 1-5.

[15] I. Ara, M. N. Hossain, and Y. S. M. Mahbub, "Baseline drift removal and de-noising of the ECG signal using wavelet transform," *International Journal of Computer Applications*, vol. 95, no.16, pp. 15-17, June. 2014.

[16] S. R. Yadhuraj, H. Harsha, K. V. Padmaja, "Removal of noise in PPG signals using wavelets," *International Journal of Computer Science and Mobile Computing (IJCSMC),* vol. 2, no. 6, pg.444 – 451, June. 2013.

[17] W. Saadeh, S. Aslam, A. Hina, and F. Asghar, "A 0.5V PPG-based Heart Rate and Variability Detection System," *IEEE Biomedical Circuits and Systems (BioCAS),* pp. 1-4, Oct. 2018.

[18] E.M.Moreno, "Non-invasive estimate of blood glucose and blood pressure from a photoplethysmograph by means of machine learning techniques," *Artificial Intelligence in Medicines, Elsevier*, vol.53, no. 2, pp. 127-138, Oct. 2011.

[19] F. Khan, U Ashraf, M. A. B. Altaf, and W. Saadeh "A Patient-Specific Machine Learning based EEG Processor for Accurate Estimation of Depth of Anesthesia," *IEEE Biomedical Circuits and Systems (BioCAS),* Oct. 2018, pp. 507-510.

[20] Y.Zhang and Z. Wang, "Non-invasive blood glucose estimation using near-infrared spectroscopy based on SVR," *IEEE 3rd Information Technology and Mechatronics Engineering Conference (ITOEC),* October. 2017, pp. 594-597.

[21] Z.Geng, F.Tang, Y. Ding, S.Li, and X.Wang, "Non-invasive glucose continuous glucose monitoring using a multisensor based glucometer and time series analysis," *Scientific Reports, Nature*, October.2017.

[22] W. Saadeh, M. A. B. Altaf, H. Alsuradi and J. Yoo, "A pseudo OFDM with miniaturized FSK demodulation body coupled communication transceiver for binaural hearing aids in 65nm CMOS," *IEEE Journal of Solid-State Circuits (JSSC)*, vol. 52, no. 3, pp 757- 768, Mar. 2017.

[23] W. Saadeh, H. Alsuradi, M. A. B. Altaf, and J. Yoo, "A 1.1mW Hybrid OFDM Ground Effect-Resilient Body Coupled Communication Transceiver for Head and Body Area Network," *in Proc. IEEE Asian Solid-State Circuits Conf. (ASSCC)*, Nov. 2016, pp. 201-204.